

STUDY ON THE EFFECTS OF DISTRIBUTION OF NEUTRON FLUX AND RELAXATION OF RESIDUAL STRESS ON IASCC CRACK GROWTH BEHAVIOUR FOR BWR REACTOR INTERNALS

Takuya Ogawa¹, Masao Itatani¹, Toshiyuki Saito², Chihiro Narazaki² and Yukiko Narahara²

¹Power and Industrial Systems Research and Development Center, Toshiba Corporation, Japan

²Isogo Nuclear Engineering Center, Toshiba Corporation, Japan

ABSTRACT

Management of plant service life is a key issue for improving the safety of light water reactors. It is known that austenitic stainless steels used for reactor internals are susceptible to irradiation-assisted stress corrosion cracking (IASCC) due to high neutron irradiation. In this study, several case studies involving structural integrity analyses for IASCC of a representative BWR core shroud by using IASCC crack growth rate curves were performed. Particularly, the effects of through-wall distribution of neutron flux and relaxation of residual stress due to irradiation creep on IASCC crack growth behaviour were investigated. IASCC crack growth rate increases with the increase of neutron irradiation and decreases with the increase of operation time due to the relaxation of residual stress. For through-wall distribution of neutron flux, flux on the outer surface of the shroud was assumed to be a quarter of that on the inner surface. Analyses were performed both by conservatively using flux on the inner surface and by using flux at the crack tip. Furthermore, relaxation behaviour of residual stress was solved by elastic-plastic-creep analysis. As a result of the case studies, it was found that considering either or both the distribution of neutron flux and the relaxation of residual stress can retard crack growth by several years. It was also found that the case considering neutron flux distribution exhibited approximately 1.5 times longer crack length than the case that did not consider neutron flux distribution when the crack depth reached 80% of the thickness, while considering residual stress relaxation provided almost the same crack length as in the case that did not consider stress relaxation.

INTRODUCTION

Plant life management is a key issue for improving the safety of light water reactors (LWRs). Core internals of LWRs are exposed to high neutron irradiation during operation. It is generally known that austenitic stainless steels used as structural materials for the core internals are susceptible to irradiation-assisted stress corrosion cracking (IASCC) due to high neutron irradiation. In boiling water reactor (BWR) plants, incidents of IASCC of core internals have been reported by the International Atomic Energy Agency (2011).

The IASCC Evaluation Guide for BWR Core Internals prepared by the Japan Nuclear Energy Safety Organization (JNES) provides structural integrity assessment methods for IASCC of BWR core internals (see Takakura et al. 2010). In our previous study (Ogawa et al. 2011), IASCC crack growth analyses for the core shroud were performed by using the IASCC evaluation guide. As a result of the study, it was found that the analysed IASCC crack growth behaviour was much more conservative compared with the actual experience of IASCC and thus improvement of the IASCC crack growth analysis procedure was recommended.

In the present study, improvement of the IASCC crack growth analysis procedure was investigated by considering through-wall distribution of neutron flux and residual stress relaxation due to irradiation creep. Several case studies of structural integrity analyses for IASCC were performed for a representative core shroud of Japanese BWRs to quantify the effect of the improvement.

CRACK GROWTH ANALYSIS METHOD

Analytical Model

A cylinder of approximately 50 mm in thickness and approximately 5000 mm in diameter was prepared as the analytical model simulating a horizontal weld of a representative BWR core shroud. The initial crack prepared on the inner surface of the model is a semi-elliptical circumferential crack of 1 mm in depth and 10 mm in length. Figure 1 shows an illustration of the analytical model with the initial crack.

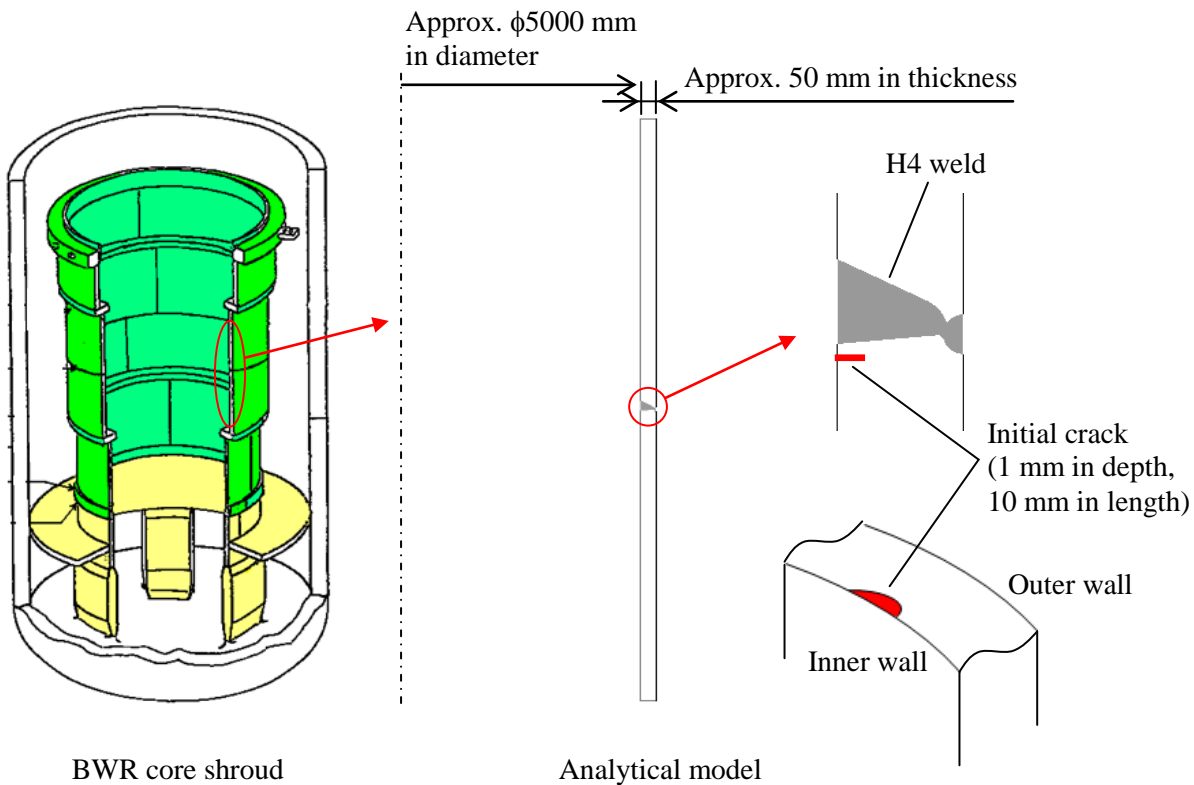


Figure 1. Analytical model with initial crack.

Analysis Conditions

Major conditions of IASCC crack growth analysis are shown below.

- Neutron flux of 1.0×10^{16} n/m²/s was used on the inner surface of the core shroud.
- Initial crack was assumed at 20, 30 or 40 years operation.
- IASCC crack growth was considered when neutron fluence was equal to or greater than 5.0×10^{24} n/m², which is one of the criteria of IASCC susceptibility in the Rules on Fitness-for-Service for Nuclear Power Plants of the Japan Society of Mechanical Engineers Code (JSME FFS Code).
- Net operating rate of 0.8 was assumed.
- Stress intensity factors K at the deepest point and at the surface point of the semi-elliptical surface crack were calculated using the equation in the JSME FFS Code, which is applicable to cases in which the normalised crack depth a/t is less than or equal to 0.8.

Weld residual stress in the analytical model was solved by the finite element method (FEM) (see Narahara et al. 2011). Relaxation of the residual stress induced by irradiation creep was solved by elastic-

plastic-creep analysis using FEM. The following creep strain equation provided in the IASCC Evaluation Guide for BWR Core Internals was used for the residual stress relaxation analysis:

$$\varepsilon_{ic} = \frac{0.19}{E} \sigma(\phi t) \quad (1)$$

where ε_{ic} is creep strain induced by neutron irradiation [mm/mm], E is Young's modulus [MPa], σ is initial residual stress [MPa], and ϕt is dose [dpa]. Figure 2 shows axial residual stress contours at the initial (unirradiated) condition and at 20, 30 and 40 years operation. Fourth polynomial curves of through-wall residual stress distribution on the through-wall line that contained the peak axial stress on the inner wall were used for IASCC crack growth analysis. Figure 3 shows the change in the fourth polynomial curves of the through-wall residual stress distribution due to neutron irradiation.

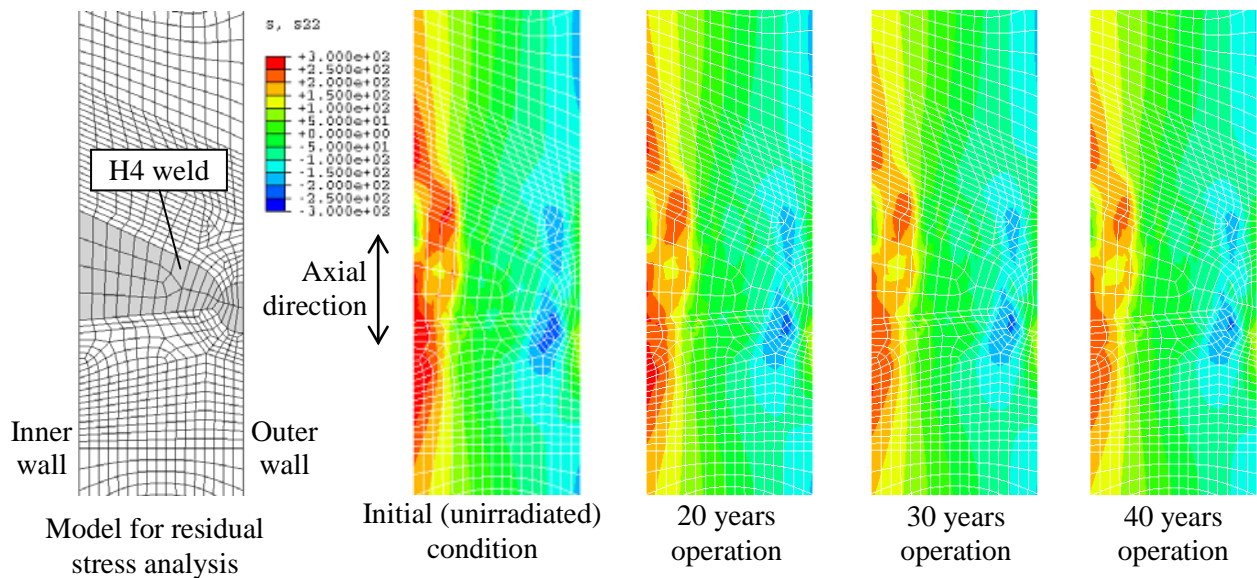


Figure 2. Axial residual stress contours by FEM.

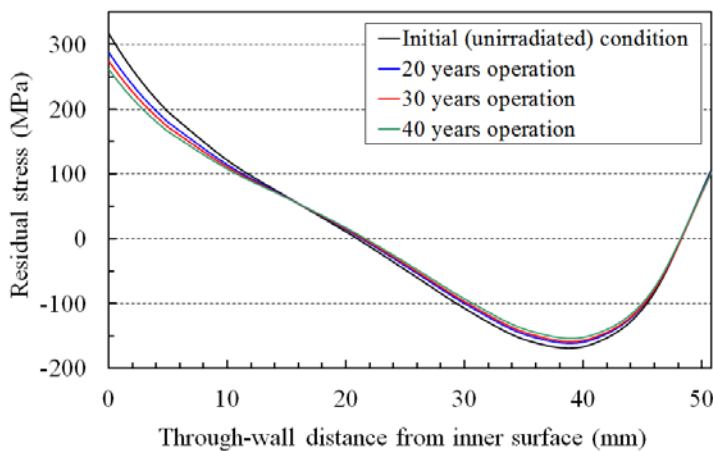


Figure 3. Change in through-wall residual stress distribution (Fourth-polynomial curves).

The IASCC Evaluation Guide for BWR Core Internals provides reference curves of IASCC crack growth rate for type 316L and type 304L stainless steels. In this study, the reference curve for type 316L stainless steel shown in equation (2) was used for IASCC crack growth analysis. In equation (2), IASCC crack growth rate depends on the stress intensity factor and the dose. The reference curve in equation (2) was formulated based on the IASCC crack growth data with the K value in the range of approximately 10 to 30 MPa√m. In this study, the reference curve in equation (2) was extrapolated to the K value in the ranges of less than 10 MPa√m and greater than 30 MPa√m. Figure 4 shows the change of relationship between IASCC crack growth rate and K value due to neutron irradiation. Crack growth rate at 60 years operation is approximately 10 times higher than that at 20 years operation.

$$\begin{aligned} da/dt &= 4.60 \times 10^{-12} \cdot K^{1.23} \cdot (\phi t)^{1.83} & (\phi t \leq 4 \text{ dpa}) \\ da/dt &= 5.85 \times 10^{-11} \cdot K^{1.23} & (4 < \phi t \leq 11 \text{ dpa}) \end{aligned} \quad (2)$$

where da/dt is IASCC crack growth rate [m/s], K is stress intensity factor [MPa√m], and ϕt is dose [dpa].

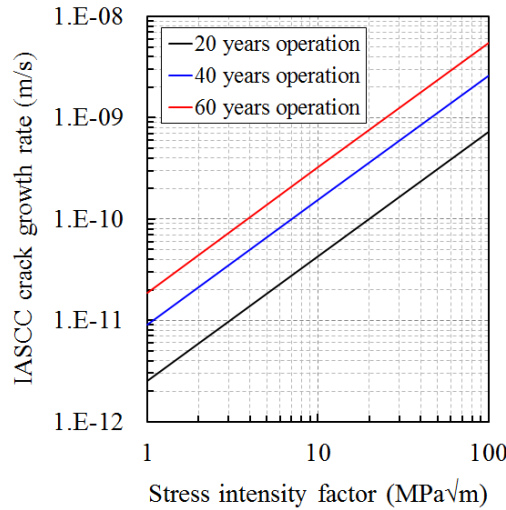


Figure 4. Change in the reference curve of IASCC crack growth rate due to neutron irradiation.

When neutron flux distribution in the core shroud was considered, neutron flux on the outer surface of the core shroud was assumed to be a quarter of that on the inner surface of the core shroud, as shown in Equation (3).

$$\phi_x = \phi_0 \cdot \exp\left(\frac{\ln 0.25}{t} \cdot x\right) \quad (3)$$

where ϕ_x is neutron flux at a distance of x from the inner surface [$n/m^2/s$], ϕ_0 is neutron flux at the inner surface [$n/m^2/s$], t is wall thickness [mm], and x is arbitrary distance from the inner surface [mm]. Figure 5 shows the neutron flux distribution assumed in the core shroud.

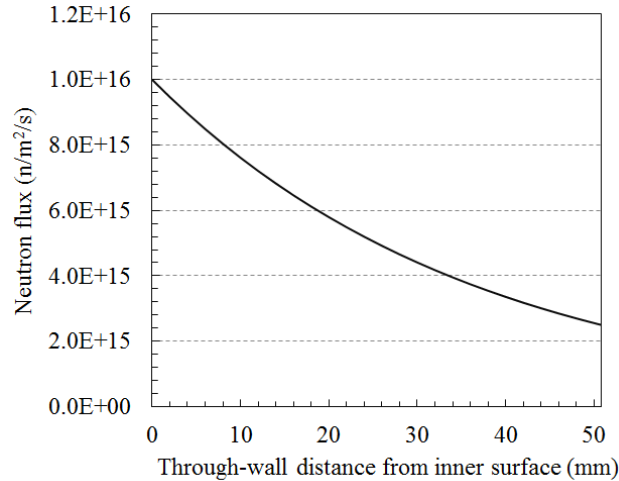


Figure 5. Neutron flux distribution assumed in the core shroud.

Analysis Procedure

Table 1 shows the matrices of IASCC crack growth analysis for investigating the effects of through-wall distribution of neutron flux and relaxation of residual stress on crack growth behaviour. Figure 6 shows the procedure for IASCC crack growth analysis. Crack growth analysis was performed by repeatedly calculating the K values and the increase of crack depth and crack length until the normalised crack depth a/t reached 0.8. When neutron flux distribution in the core shroud was considered, neutron fluence at the crack tip was evaluated based on neutron flux at the crack tip. Otherwise, neutron fluence at the crack tip was evaluated based on neutron flux on the inner surface. When residual stress relaxation due to irradiation creep was considered, residual stress according to operating time was used to calculate the K values. Otherwise, only residual stress in the initial (unirradiated) condition was used. Repetitive crack growth calculation shown in Figure 6 was run by in-house code programmed by Microsoft Excel® 2010 Visual Basic for Applications (VBA).

Table 1: IASCC crack growth analysis matrices.

Case ID	Initial crack assumption	Neutron flux distribution	Residual stress relaxation
20-A	At 20 years operation	No distribution	No relaxation
20-B		With distribution	No relaxation
20-C		No distribution	With relaxation
20-D		With distribution	With relaxation
30-A	At 30 years operation	No distribution	No relaxation
30-B		With distribution	No relaxation
30-C		No distribution	With relaxation
30-D		With distribution	With relaxation
40-A	At 40 years operation	No distribution	No relaxation
40-B		With distribution	No relaxation
40-C		No distribution	With relaxation
40-D		With distribution	With relaxation

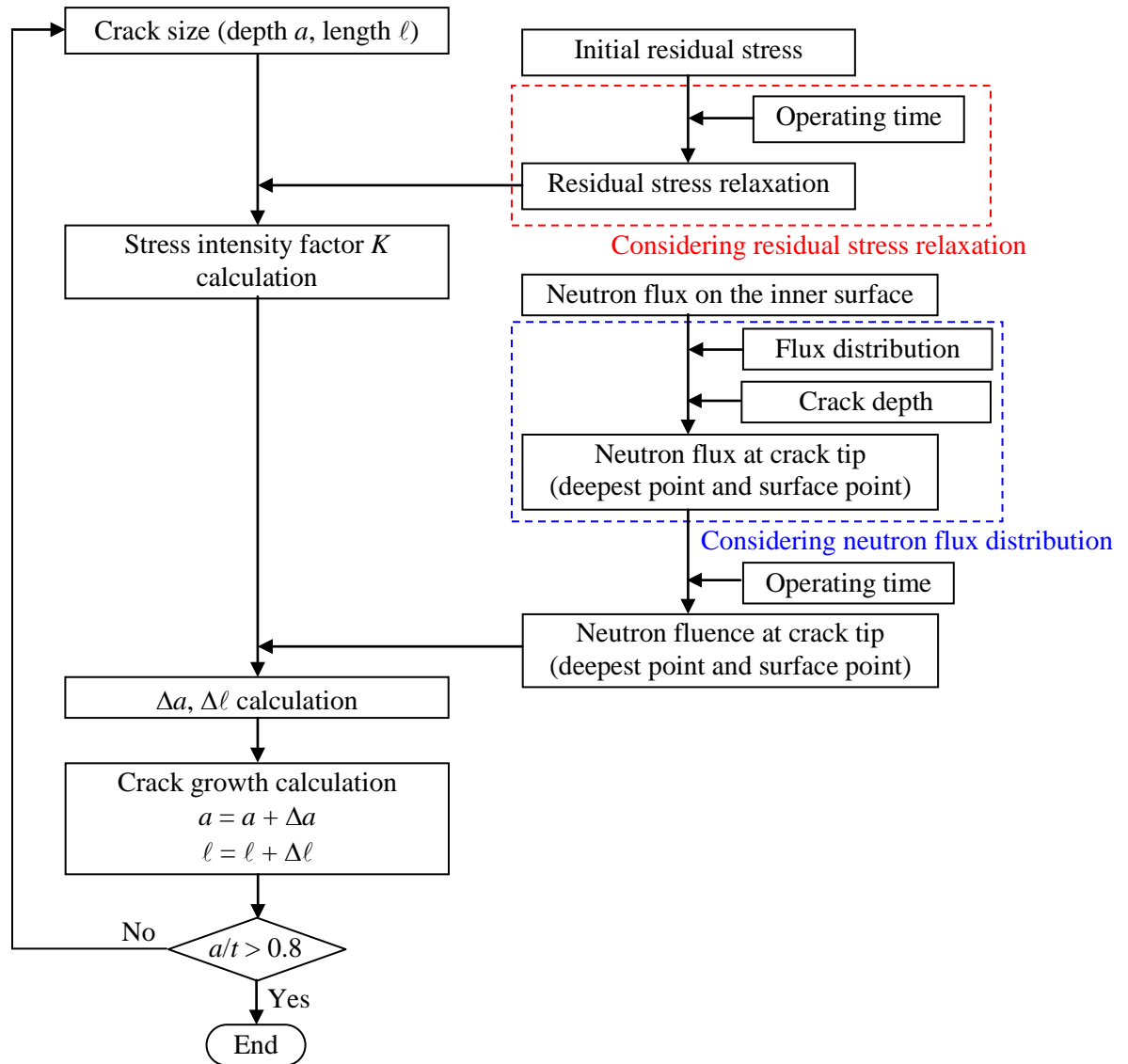


Figure 6. IASCC crack growth analysis flow.

CRACK GROWTH ANALYSIS RESULTS AND DISCUSSION

Analysis Results

The relationship between crack depth a and operating time for each case with an initial crack at 20, 30 or 40 years operation is shown in Figures 7, 8, and 9, respectively, and the results are summarised in Table 2. The cases in which an initial crack was assumed at 40 years operation provide a shorter crack growth period than in the cases of an initial crack at 20 or 30 years operation. This is because the higher operating time resulted in a higher IASCC crack growth rate curve due to high neutron fluence. A comparison of the Case A and Case B series revealed that considering neutron flux distribution provided 1.9 to 2.8 years longer crack growth period, and it was most effective in the cases of an initial crack at 40 years operation. On the other hand, a comparison of the Case A and Case C series revealed that considering residual stress relaxation provided 1.7 to 1.9 years longer crack growth period, and it hardly depended on when the

initial crack was assumed. The longest crack growth period was provided by the Case D series that considered both neutron flux distribution and residual stress relaxation.

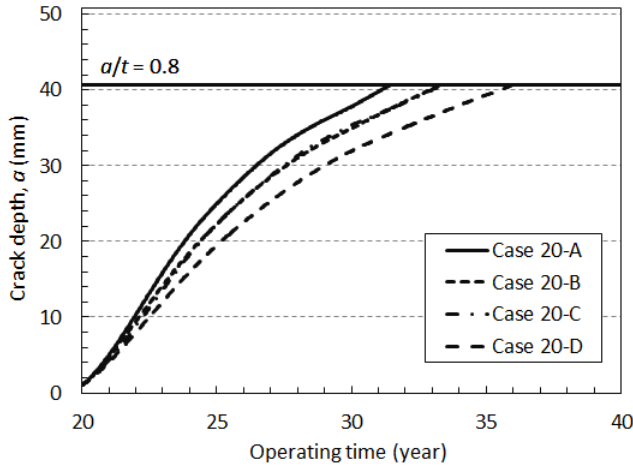


Figure 7. Relationship between crack depth a and operating time with initial crack at 20 years operation.

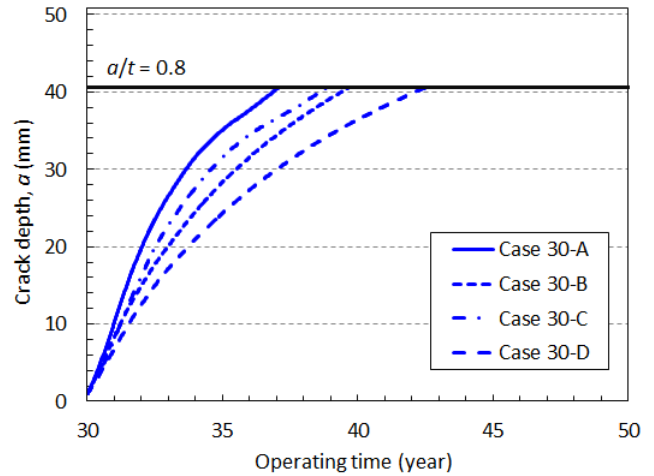


Figure 8. Relationship between crack depth a and operating time with initial crack at 30 years operation.

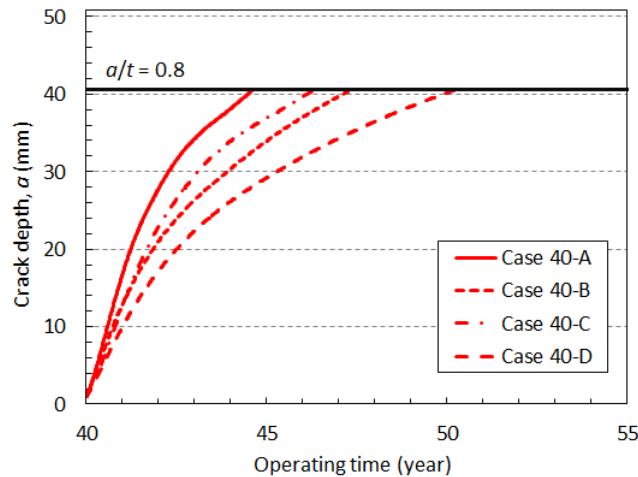


Figure 9. Relationship between crack depth a and operating time with initial crack at 40 years operation.

Effect of Neutron Flux Distribution

The effect of considering neutron flux distribution on crack growth behaviour was investigated by a comparison of Case 40-A and Case 40-B. Figure 10 shows the relationship between crack depth a and crack length ℓ , and Figure 11 shows the relationship between crack depth a and the K value at the deepest point. As shown in Figure 9, through-wall crack growth was retarded by considering neutron flux distribution because it gave a lower neutron flux at the deepest point compared with Case 40-A. It was found, however, that Case 40-B provided approximately 1.5 times longer crack length than in Case 40-A when the crack depth reached 80% of the thickness, as shown in Figure 10. Therefore, the crack in Case 40-B had a larger K value at the deepest point than that of Case 40-A since the crack size of Case 40-B was relatively large.

Table 2: Summary of IASCC crack growth behaviour.

Case ID	Year with an initial crack (year)	Year with crack a/t greater than 0.8 (year)	Crack growth period (years)	Increase in crack growth period compared with Case A series (years)
20-A	20	31.4	11.4	-
20-B		33.3	13.3	1.9
20-C		33.3	13.3	1.9
20-D		36.0	16.0	4.6
30-A	30	37.1	7.1	-
30-B		39.7	9.7	2.6
30-C		38.9	8.9	1.8
30-D		42.5	12.5	5.4
40-A	40	44.6	4.6	-
40-B		47.4	7.4	2.8
40-C		46.3	6.3	1.7
40-D		50.3	10.3	5.7

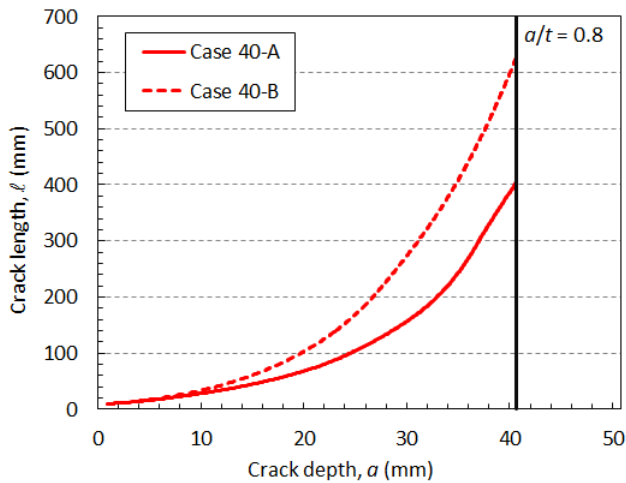


Figure 10. Relationship between crack depth a and crack length l in Cases 40-A and 40-B.

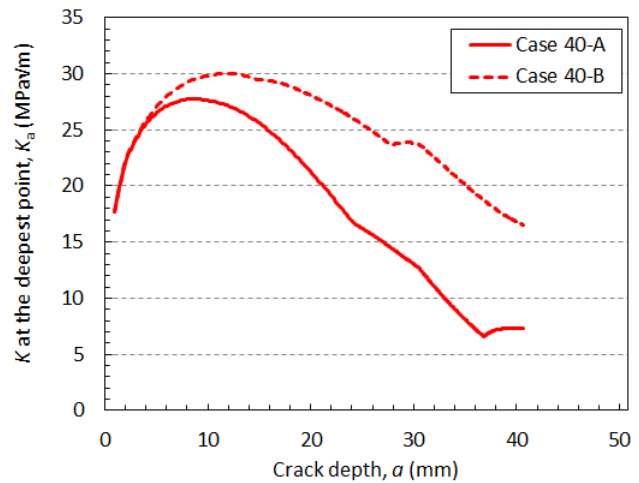


Figure 11. Relationship between crack depth a and K value at the deepest point in Cases 40-A and 40-B.

Effect of Residual Stress Relaxation

The effect of considering residual stress relaxation on crack growth behaviour was investigated by a comparison of Case 40-A and Case 40-C. Figure 9 indicates that considering residual stress relaxation can retard through-wall crack growth. Here, considering residual stress relaxation provides almost the same crack length behaviour as in Case 40-A unlike the case of considering neutron flux distribution, as shown in Figure 12. Figures 13 and 14 show the K value at the deepest point and at the surface point, respectively. It was confirmed that both K values of Case 40-C were much smaller than those of Case 40-A, and this was due to stress relaxation.

According to Figures 13 and 14, the K value at the deepest point was in the range of approximately 5 to 30 $\text{MPa}\sqrt{\text{m}}$, and that at the surface point was in the range of approximately 5 to 65 $\text{MPa}\sqrt{\text{m}}$. In this study, the IASCC crack growth rate curve for the K value in the ranges of less than 10 $\text{MPa}\sqrt{\text{m}}$ and greater than 30 $\text{MPa}\sqrt{\text{m}}$ was extrapolated. Further investigation of the adequacy of the extrapolation is needed

particularly in the range of K value greater than $30 \text{ MPa}\sqrt{\text{m}}$. It is expected that an increase of crack length will be retarded if there is an upper rate of IASCC crack growth like the intergranular stress corrosion cracking (IGSCC) crack growth rate curves in the JSME FFS Code.

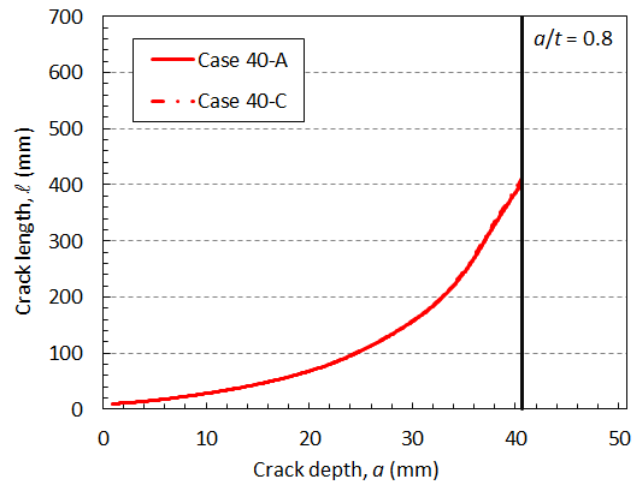


Figure 12. Relationship between crack depth a and crack length ℓ in Cases 40-A and 40-C.

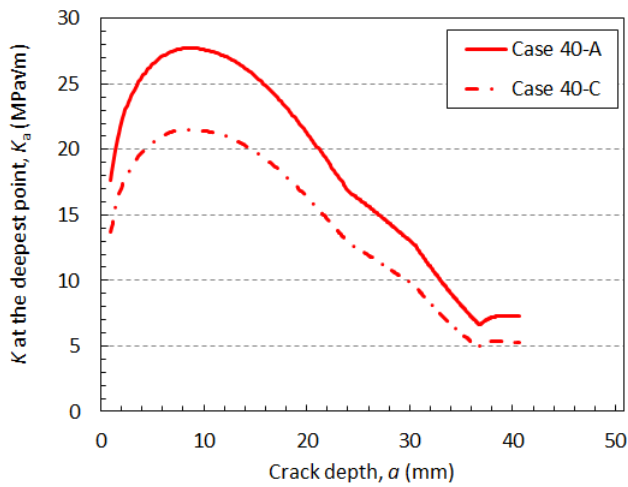


Figure 13. Relationship between crack depth a and K at the deepest point in Cases 40-A and 40-C.

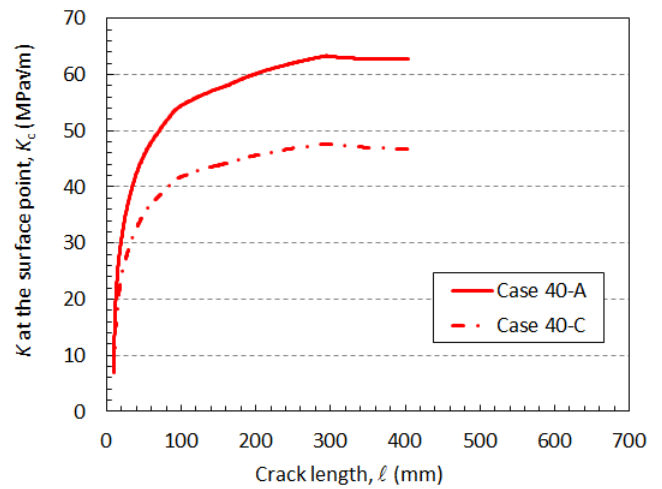


Figure 14. Relationship between crack length ℓ and K at the surface point in Cases 40-A and 40-C.

NOMENCLATURE

a	Crack depth [mm]
Δa	Increase of crack depth [mm]
ℓ	Crack length [mm]
$\Delta \ell$	Increase of crack length [mm]
t	Wall thickness [mm]
a/t	Normalised crack depth
K	Stress intensity factor [$\text{MPa}\sqrt{\text{m}}$]
ϕ	Neutron flux [$\text{n}/\text{m}^2/\text{s}$]
ϕt	Neutron fluence [n/m^2], Dose [dpa] ($1 \text{ dpa} = 7.0 \times 10^{24} \text{ n}/\text{m}^2$)

da/dt	IASCC crack growth rate [m/s]
ε_c	Creep strain induced by neutron irradiation [mm/mm]
E	Young's modulus [MPa]
σ	Initial residual stress [MPa]

CONCLUSION

An IASCC crack growth analysis procedure that considers either or both through-wall distribution of neutron flux and residual stress relaxation due to irradiation creep was investigated. Several case studies of structural integrity analysis for IASCC were performed for a representative core shroud of Japanese BWRs to quantify the effects. Residual stress relaxation was solved by elastic-plastic-creep analysis using FEM. Neutron flux on the outer surface was assumed to be a quarter of that on the inner surface. The IASCC crack growth rate curve for 316L stainless steel in the IASCC Evaluation Guide for BWR Core Internals was used for crack growth analyses.

As a result of the case studies, it was found that considering either or both through-wall distribution of neutron flux and residual stress relaxation can retard through-wall crack growth by several years. However, it was also found that considering neutron flux distribution resulted in approximately 1.5 times longer crack length than in the case that did not consider neutron flux distribution when the crack depth reached 80% of the thickness, while considering residual stress relaxation could provide almost the same crack length as in the case that did not consider stress relaxation. Further investigation of the adequacy of the extrapolation of IASCC crack growth rate is needed in the future.

REFERENCES

- International Atomic Energy Agency (2011). "Stress Corrosion Cracking in Light Water Reactors: Good Practices and Lessons Learned," IAEA Nuclear Energy Series Technical Reports No. NP-T-3.13.
- Takakura, K., Tanaka, S., Nakamura, T., Chatani, K. and Kaji, Y. (2010). "IASCC Evaluation Method for Irradiated Core Internal Structures in BWR Power Plants," *Proc. ASME 2010 Pressure Vessels & Piping Division / K-PVP Conference*.
- Ogawa, T., Narahara, Y., Narazaki, C., Itatani, M., Murofushi, T., Saito, T. and Takakura, K. (2011). "Study on Structural Integrity Assessment for IASCC of BWR Plants – (2) Fracture Mechanics Investigation for IASCC Crack Growth in Core Shroud Structure," *JSME M&M2011 Conference*, OS2506.
- The Japan Society of Mechanical Engineers (2012). *Codes for Nuclear Power Generation Facilities – Rules on Fitness-for-Service for Nuclear Power Plants*, JSME S NA 1-2012.
- Narahara, Y., Murofushi, T., Narazaki, C., Ogawa, T., Itatani, M., Saito, T. and Takakura K. (2011). "Study on Structural Integrity Assessment for IASCC of BWR Plants – (1) Evaluation of Residual Stress Relaxation Induced by Irradiation in Core Shroud Structure," *JSME M&M2011 Conference*, OS2505.